Article

In Silico Exploration for New Antimalarials: Arylsulfonyloxy Acetimidamides as Prospective Agents

Saroj Verma,[†] Utsab Debnath,[†] Pooja Agarwal,[‡] Kumkum Srivastava,[‡] and Yenamandra S. Prabhakar*[,†]

[†]Medicinal and Process Chemistry Division, [‡]Parasitology Division, CSIR-Central Drug Research Institute, Jankipuram Extension, Lucknow-226 031, India

Ⓢ Supporting Information

ABSTRACT: A strategy is described to identify new antimalarial agents to overcome the drug resistance and/or failure issues through in silico screening of multiple biological targets. As a part of this, three enzymes namely CTPS, CK, and GST were selected, from among 56 drug targets of *P. falciparum*, and used them in virtual screening of ZINC database entries which led to the design and synthesis of arylsulfonyloxy acetimidamides as their consensus inhibitors. From these, two compounds showed good activity against sensitive (3D7; IC$_{50}$, 1.10 and 1.45 μM) and resistant (K1; IC$_{50}$, 2.10 and 2.13 μM) strains of the parasite, and they were further investigated through docking and molecular dynamics simulations. The findings of this study collectively paved the way for arylsulfonyloxy acetimidamides as a new class of antimalarial agents.
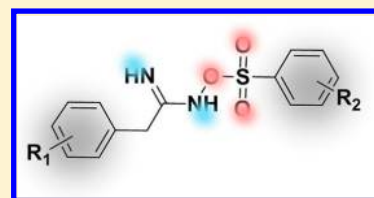
1. INTRODUCTION

Worldwide malaria maps with poverty. This protozoan infection is a leading cause of morbidity and mortality in tropical and subtropical regions. Globally it alone causes a disease burden of about 200 million infections and more than 500 000 deaths annually.[1] Different Plasmodium species which include *P. falciparum*, *P. malariae*, *P. vivax*, and *P. ovale* are the causative agents. Among these, *P. falciparum* (*Pf*) is the most lethal and widely spread in human beings. Its clinical management depends on several drugs.[2] They include chloroquine (CQ), mefloquine, atovaquone, proguanil, sulphadoxine−pyrimethamine combination, artemisinins, artemisinin combination therapy, etc. Apart from the foregoing, some widely tried procedures for discovering fresh leads/drugs against this parasite include screening of diverse chemicals, new combinations of two (or more) existing drugs to act on same or different enzyme targets and strategies to counter the drug resistance.[2−4] In the face of these interventional measures malarial parasite, with impunity, has managed to keep the drugs at bay in controlling its rise and transmission.[2] The treatment failures are often attributed to a multitude of reasons which include mutation of targeted enzyme(s), amplification of parasite's transport proteins in pumping out or expelling the drug(s), and/or opening up of alternative biochemical/metabolic paths in the organism for its survival.[5,6] The situation calls for rethinking and conceptualization of strategies to interfere with the deep-seated pathways of the parasite to restrain its resurgence and control it with little scope for the emergence of drug-resistant strains. In this outset, exploring the parasite's biological machinery for hitherto unexplored biochemical pathways may open up fresh and tactical avenues for new chemicals to combat the malaria.

The therapeutic strategies aiming at single biological target (of the pathogen) with limited or closely related chemical entities are often attributed to be a leading cause for the drug failure and/or emergence of drug resistant strains of pathogens.[5,6] Among the feasible options to deal with the situation, the strategies mulling over "multiple drugs against single or multiple targets" (or combination therapy)[2] and "single drug against multiple targets"[3,4] are the notable ones. While the former one is fairly explored in the chemotherapy of infectious diseases with limited success, the later one holds promise for exploration. The main causative agent of human malaria, *P. falciparum*, with its 14 chromosomes encodes more than five thousand proteins.[7] It is a huge reservoir to explore all probable targets of antimalarial drugs. Even though every organism tanks large number of enzymes and proteins as part of its biochemical machinery, its survival and sustenance depends on the function of a few key ones in the regulatory network. In this backdrop a computational approach is contemplated to identify multiple enzymes to design single consensus chemical entity (CCE) as their inhibitors/modulators to overcome the treatment failure and emergence of drug resistance in malaria.

Some connectedness among possible drug targets together with their functional importance in biochemical/metabolic paths may offer scope for the selection of potential enzymes and thereby the design of CCEs as their inhibitors/modulators. The concept is explored through a distance matrix approach by identifying three key enzymes of the parasite which have vital functions in the biochemical/metabolic network. This has resulted in cytidine triphosphate synthetase (CTP synthetase or CTPS),[8] choline kinase (CK),[9] and glutathione S-transferase (GST)[10] as potential enzymes for exploring the concept of a single drug against multiple targets or CCE. Furthermore, the pathways of these enzymes, as indicated in Brenda enzyme database, suggested their significance to the parasite's sustenance.[11] They are used in virtual screening of ZINC database entries[12] to identify the CCEs. This has led to

arylsulfonyloxy acetimidamides as model compounds for synthesis and biological evaluation. Some of these compounds showed encouraging activity against *P. falciparum* (3D7, K1). The most active compound from these is further studied through docking[13,14] and molecular dynamic (MD) simulations[15] to shed some light on possible molecular interactions with the selected enzymes. The details are discussed here.

2. MATERIALS AND METHODS

2.1. Enzyme Database. The study has involved fifty-six drug targets of *P. falciparum* reported in recent literature (Table 1). The availability of primary structures (FASTA sequences) and a precedence/proposal for them as probable drug targets was the criteria for the consideration of these enzymes. It is assumed that from among these enzymes, the "connected and proximately placed" ones give scope to design a CCE to modulate their activity. Thus, we formulated a strategy, akin to phylogenic

Table 1. *P. falciparum* Enzymes Considered in the Exploration

S. no.	targets[a]	S. no.	targets[a]
1	cytochrome c oxidase	29	farnesyltransferase
2	1-deoxy-D-xylulose 5-phosphate reducto-isomerase	30	glutathione S-transferase
3	deoxyhypusine synthase	31	β-ketoacyl-ACP synthase
4	dihydrofolate reductase	32	N-myristoyltransferase
5	dihydroorotate dehydrogenase	33	cholinephosphate cytidylyltransferase
6	enoyl-ACP-reductase	34	hypoxanthine guanine phospho ribosyl-transferase
7	ferredoxin NADP reductase	35	choline kinase
8	glutamate dehydrogenase	36	dihydropteroate synthase
9	glutathione reductase	37	hexokinase
10	lactate dehydrogenase	38	homospermidine synthase
11	ubiquinol-cytochrome-c reductase	39	S-adenosylmethionine synthetase
12	ribonucleotide reductase	40	aspartate carbamoyltransferase
13	succinate dehydrogenase	41	1-deoxy-D-xylulose-5-phosphate synthase
14	thioredoxin reductase	42	purine nucleoside phosphorylase
15	DNA gyrase	43	plasmepsin I
16	peptidyl-prolyl *cis−trans* isomerase	44	plasmepsin II
17	topoisomerase I	45	sphingomyelinase
18	topoisomerase II	46	adenosine deaminase
19	triose phosphate isomerase	47	histone deacetylases
20	adenylosuccinate lyase	48	S-adenosyl-L-homocysteine
21	β-hydroxyacyl-ACP dehydratase	49	peptide deformylase
22	chorismate synthase	50	helicase
23	DNA-(apurinic/apyrimidinic site) lyase	51	dihydroorotase
24	fructose 1,6 biphosphate aldolase	52	acyl-CoA synthetase
25	2-C-methyl-D-erythritol-2,4-cyclodiphosphate synthase	53	CTP synthase
26	orotate phosphoribosyltransferase	54	carbamoyl phosphate synthetase
27	RNA polymerase	55	dihydrofolate synthase
28	DNA polymerase	56	acetyl-CoA carboxylase Ligase

[a]The enzymes listed under serial numbers 1−14 are oxidoreductases (Ox), 15−19 are isomerases (Is), 20−25 are lyases (Ly), 26−42 are transferases (Tr), 43−51 are hydrolases (Hy), and 52−56 are ligases (Li). Complete bibliographic details are provided in the Supporting Information.

analysis, for the selection of three enzymes from among the considered targets by a distance matrix approach and by examination of their functional roles in the metabolic pathways.

2.2. Selection of Target Enzymes. The study has proceeded with segregation of all the targets into six distinct enzyme classes (Table 1). The FASTA sequences of all the targets were retrieved from NCBI and UniProt. The BLAST (Basic Local Alignment Search Tool) analysis of FASTA sequences of all targets was carried out to identify the connectedness and proximity of the targets. The sequence similarity of each target was determined against all others in terms of e-values. These were used to compute the total distance (TD) and average distance (AD) of targets, between different classes (*inter*; BC) as well as within each class (*intra*; C), as described below.

$$\mathrm{TD_{BC}} = \sum e_{i,j}$$

$$\mathrm{AD_{BC}} = \sum e_{i,j}/(nm)$$

where, $\mathrm{TD_{BC}}$ is between classes total distance, $\mathrm{AD_{BC}}$ is between classes average distance, $e_{i,j}$ is the e-value between target i ($i = 1−n$; n is total targets in *p*-class) of *p*-class and target j ($j = 1−m$; m is total targets in *q*-class) of *q*-class.

$$\mathrm{TD_C} = \sum e_{i,j}$$

$$\mathrm{AD_C} = \sum e_{i,j}/((n^2 − n)/2)$$

where, $\mathrm{TD_C}$ is within class total distance, $\mathrm{AD_C}$ is within class average distance, $e_{i,j}$ is the e-value between targets i and j with i varying from 1 to n and j varying from $i + 1$ to n; n is the total targets in the class.

In the first iteration, the enzyme class with smallest average in-between class distances ($\mathrm{AD_{BC}}$) was considered and assigned as closely placed to all others (complete data is provided as part of the Supporting Information). The first enzyme of intended multiple targets was selected from among the members of this class using the within class distances as well as its relevance in the metabolic pathway for the parasite's survival and sustenance. In the second iteration, the first target was taken as reference to compute the distances of remaining classes from it and the class which is closely placed to it was considered for further analysis. In view of the importance of "cleaning up" or "detoxification" processes in parasite milieu, *P. falciparum* glutathione S-transferase (GST) is adopted as third enzyme of the intended multiple targets for inhibition/modulation.

2.3. Structural Modeling. The FASTA sequence of target protein was retrieved from the NCBI database and its primary properties were assessed using different servers.[16,17] The template protein structure(s) consensus to target sequence was searched from the protein data bank with PSI-BLAST,[18] PHYRE[19] and JPred3[20] under default parameter settings. The templates showing low e-value and high sequence identity with the target sequence were selected as model template(s). The alignment of target sequence with the template was done using Modeler 9.10.[21] On alignment the disordered regions of target were checked in DisEMBL.[22] Giving due consideration to the conserved motifs, the disordered regions of the aligned target was rectified in Bio-Editor[23,24] by editing the sequence to minimize the gaps/insertions. The "rectified" target sequence was realigned with the template in Modeler 9.10 to generate the initial models. The model(s) was assessed for the stereochemical quality scores which include DOPE score, MOLPDF, GA341

Table 2. Average Distance of Enzyme Classes Based on the *e*-Values between Targets of *P. falciparum*[a]

enzyme class	oxidoreductase	isomerase	lyase	transferase	hydrolase	ligase
oxidoreductase	2.56					
isomerase	2.95	3.40				
lyase	2.89	2.71	1.47			
transferase	2.32	2.61	2.18	2.25		
hydrolase	2.40	2.67	2.46	2.09	2.60	
ligase	2.18	2.51	2.30	1.86	1.86	1.11

[a]All enzymes and corresponding data are provided in the Supporting Information.

score, Ramachandran plot, Errat plot, and Prosa plot, and the best scored one was selected for refinement.[21,25,26] This was further refined for relieving steric clashes and improper contacts by energy minimization using GROMOS96 force field[27] in Swiss PDB viewer 4.0.1,[28] followed by iterative loop refinement in Modeler 9.10 (ERRAT plot showing confidence limits to reject residue regions that exceed ≥95%) to give the homology model of the target. Followed by this, the active site(s) (binding pocket) of selected targets were identified with due consideration to the bound ligands of template protein(s) and the conserved domain by involving the CASTp (Computed Atlas of Surface Topology of Proteins), Site-finder of MOE, and protomol of SYBYLX 1.3.

2.4. Molecular Dynamics (MD) Simulations. In NAMD2.7[15] MD simulations were carried out on the homology model to obtain equilibrated protein structure. This was done under periodic boundary conditions using the solvated (water box) protein by applying appropriate force field, constant molecular number, pressure (1 atm), temperature (310 K; NPT), cut-offs for nonbonded atom interactions (12 Å), and Particle mesh Ewald (PME) algorithm for long-range electrostatic forces between the atoms. The system (protein in water box) was adequately minimized followed by equilibrated for enough length of time. The integration time step of dynamics was set to 2 fs, and the trajectories were collected at regular intervals. The results were analyzed and protein stability was assessed in VMD 1.91 (Visual molecular dynamics),[29] VEGAZZ,[30] and Video match[31] by computing different parameters which include, energies, radius of gyration, and root-mean-square deviation (RMSD) of the trajectories. Furthermore, the MD simulations were also suitably carried out on the selected enzymes and CCE complexes to study the stability of these systems and dynamics of molecular interactions between them.

2.5. Virtual Screening. From ZINC database, using the structural similarity between its entries and the known substrates/inhibitors of *Pf*-CTPS, CK, and GST, 8635 molecules were identified for virtual screening. The identified molecules were screened against the selected targets in the Surflex-Dock Geomax (SFXC) module of Sybyl-X 1.3.[13] The corresponding proteins were prepared following the default procedure set in the module by applying the Gasteiger–Huckel charges and subjected to staged energy minimization using Tripos force field. The residue based protomols (binding pockets) were generated from the prepared proteins for the docking experiments. The screening of the identified molecules was done by successively docking them into the generated binding pockets. The affinities of the molecules to the respective enzymes were analyzed using crash, polar, and total scores obtained from the docking experiments.

2.6. Synthesis. The arylsulfonyloxy acetimidamides, the designed common inhibitors of three targets, are prepared using the following synthetic scheme.[32]

2.6.1. Synthesis of N′-Hydroxy-2-arylacetimidamides (2). Hydroxylamine hydrochloride (2.4 mmol) was dissolved in methanol. Methanolic sodium methoxide (2.5 mmol) was added to this solution and refluxed for 30 min. 4-Substituted benzeneacetonitraile (2 mmol) (**1**) was added to this solution and further refluxed the contents for 12 hours to yield corresponding N′-hydroxy-2-arylacetimidamide (**2**). The progress of the reaction was monitored by TLC (10% MeOH/ CHCl$_3$). On completion of the reaction, methanol was evaporated by rota vapor under reduced pressure. The residue was dissolved in dichloromethane and washed with brine. The organic layer was collected and dried with anhydrous sodium sulfate to obtain crude compound 2 (yield 75−79%). This was further purified through column chromatography and the structure of N′-hydroxy-2-arylacetimidamide (**2**) was confirmed by analyzing NMR and mass spectra.

2.6.2. Synthesis of Arylsulfonyloxy Acetimidamides (3). In a round-bottom flask to 30 mL dichloromethane, 1 mmol of compound **2** followed by 1.2 mmol triethayl amine were added and the solution was cooled to 0 °C. To this, 1.2 mmol arylsulphonyl chloride was added with constant stirring. The stirring of reaction mixture was continued for 1−2 h to complete the sulfonylation of **2** to afford corresponding arylsulfonyloxy acetimidamide (**3**). The completion of reaction was monitored through TLC (40% EtOAc/hexane). On completion of reaction, the mixture was washed with brine and dried with anhydrous sodium sulfate followed by evaporated dichloromethane under reduced pressure to obtain crude arylsulfonyloxy acetimidamide (**3**) (yield 70−85%). This was further purified through column chromatography and the structure of arylsulfonyloxy acetimidamide (**3**) was confirmed by analyzing ^{1}H NMR, ^{13}C, ES-MS, and HRMS spectra.

2.7. Biological Screening. The synthesized compounds were evaluated for antimalarial activity against 3D7 (CQ-sensitive) and K1 (CQ-resistant) strains of *P. falciparum* using Malaria SYBR Green I nucleic acid staining dye based fluorescence (MSF) assay as mentioned by Singh et al.[33] The stock (10 mM) solution was prepared in DMSO and test dilutions were prepared in culture medium (RPMI-1640-FBS). Chloroquine-diphosphate (SIGMA) was used as reference drug. Briefly the procedures are described below.

2.7.1. Antimalarial Assay. 50 μL of culture medium was dispensed in 96 well plate followed by addition of 50 μL of highest concentration (in subsequent screens with 2-fold serial dilutions) of test compounds (in duplicate wells) in row B. Following this, 50 μL of 2.0% parasitized cell suspension containing 0.8% parasitaemia (Asynchronous culture containing more than 80% ring stages) was added to each well except four wells in row "A" which received matching volume of non parasitized erythrocyte suspension. The plates were incubated at 37 °C in CO$_2$ incubator in an atmosphere of air mixture with 5% CO$_2$ for 72 h. Following this 100 μL of lysis buffer containing 2×

concentration of SYBR Green-I (Invitrogen) was added to each well and the plates were incubated for one more hour at 37 °C. The plates were examined at 485 ± 20 nm (excitation) and 530 ± 20 nm (emission) for relative fluorescence units (RFUs) per well using the fluorescence plate reader (FLX800, BIOTEK). The IC_{50} values were obtained by Logit regression analysis of dose response curves using a preprogrammed Excel spreadsheet.

2.7.2. Cytotoxicity Assay. Cytotoxicity of the compounds was determined using Vero cell line (C1008; Monkey kidney fibroblast) following the method as mentioned in the work of Sharma et al.[34] The cells were incubated with compound-dilutions for 72 h and MTT (SIGMA) was used as reagent for detection of cytotoxicity. Podophyllotoxin (SIGMA) was used as the reference drug. The 50% cytotoxicity concentration (CC_{50}) was determined using nonlinear regression analysis of dose response curves using a preprogrammed Excel spreadsheet.

3. RESULTS AND DISCUSSION

3.1. Target Selection. The average in-between class distances of six distinct enzyme classes comprising fifty-six drug targets of *P. falciparum* are shown in Table 2 (Figure 1).
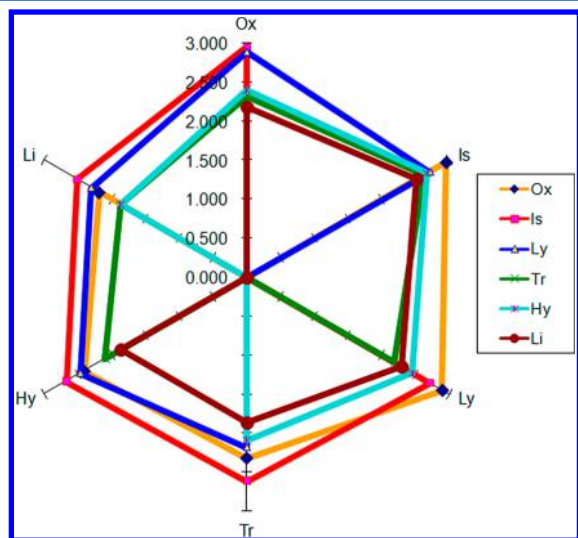

Figure 1. Interclass distances (*e*-value) of *P. falciparum* targets.

This clearly showed that ligase is "closely" placed to all other classes ($\sum AD_{BC} = 10.70$). This class has five enzymes in it. The within class distances of each enzyme with all other targets led to CTP synthase (CTPS) as closely placed one to remaining members of this class. In the parasite's metabolic pathway, CTPS is involved in the synthesis of CTP, a high-energy molecule like ATP. The parasite uses CTP in the synthesis of glycerophospholipids and glycosylation of proteins and as a substrate in RNA synthesis. In view of this, CTPS has been selected as one of the three intended targets for inhibition/modulation.

For the selection of next target, CTPS has been taken as the focal point to compute the distances between CTPS and remaining five enzyme classes. Herein, the transferases have emerged as close to CTPS. This enzyme class has 17 targets in it. The search for second enzyme in this class in conjunction with CTPS has led to choline kinase (CK) as potential target. In the parasite CK facilitates the biosynthesis of phospholipid (PL) through the phosphorylation of choline. In the metabolic pathway by making use of CTP, choline monophosphate gets converted into corresponding diphosphate nucleotides (CDP-

choline) followed by to phosphatidylcholine. Interestingly, for the parasite ethanolamine kinase (EK) is another enzyme in its pathway for the production of phosphatidylethanolamine via CTP.

For all organisms/living systems, cleaning up or detoxification of its milieu is an important task. In the parasite, glutathione S-transferase (GST) is one enzyme involved in the detoxification process via ceramide. As a part of downstream regulation of events sphingomyelin synthase (SS) oversees the formation of sphingomyelein from ceramide and phosphatidylcholine (from CK/CTPS pathway) and pave the way for detoxification/apoptosis signaling in the parasite. In the process, parasite's GST facilitates the glutathione-toxin (ceramide/xenobiotics) adduct formation and helps in detoxification of the milieu. Thus, inhibition of GST may help in the retention of ceramide/xenobiotic substances thereby make the parasite milieu toxic. Considering this we have adopted parasite's GST as third enzyme of the intended multiple targets for inhibition. The interconnections between the biochemical pathways of selected enzymes are shown in Figure 2, thus justifying them as possible targets against malaria.

3.2. *Pf*-CTPS Homology Model. In the absence of the 3D structure of *Pf*-CTPS, its homology model has been developed from the FASTA sequence (860 residues) with accession code AAC36385 retrieved from the NCBI database.[8] It is a 98.85 kDa protein with isoelectric point 6.381. Its secondary structure membrane topology showed that the residues are distributed in the cytoplasmic (1−520), transmembrane (521−539), and extra-cyoplasmic (540−860) regions. It has two substrate binding domains namely synthetase domain in vicinity of N-terminal and glutaminase domain in vicinity of C-terminal. Using the glutaminase domain, *Pf*-CTPS transforms uridine-5′-triphosphate (UTP) into cytidine triphosphate (CTP).

A standard search of protein data bank with the *Pf*-CTPS FASTA sequence led to the X-ray structures of CTPS from *sulfolobus solfataricus* (PDB code: 3NVA; number of residues, 535; *e*-value, 7.00×10^{-107}; sequence identity, 39%)[35] and *Thermus thermophilus* (PDB code: 1VCO; number of residues, 550; *e*-value, 9.00×10^{-102}; sequence identity, 36%)[36] as best consensus templates for its homology modeling. A further examination of *Pf*-CTPS sequence in PHYRE, a fold recognition method, suggested 3NVA as best suited template for the structural modeling of this protein. In Modeler 9.10 the alignment of target FASTA sequence with the 3NVA template followed by the editing of undefined portions with due care for the conserved regions and on iterative refinement led to the optimized homology model of *Pf*-CTPS (Figure 3). We also made attempts to model the *Pf*-CTPS using 3NVA, 1VCO, and other pdb templates, through multiple sequence alignment; however, they did not give any better results than using 3NVA alone. In this scenario, we carried out the further study using the *Pf*-CTPS model generated from 3NVA. The model is further refined through MD simulations for 5 ns. The structure has reached an equilibrium conformation approximately after 0.75 ns of dynamics simulations. The last frame has shown RMSD 4.87 Å (for frames from 0.75 to 5 ns, average RMSD $\pm$ SD is 4.39 ± 0.28 Å). On reaching equilibrium, the model has retained its shape without much change in its structure (Figure 3).

3.3. Target Sites. In *Pf*-CTPS, as the glutaminase domain is important for the transformation of UTP into CTP, in the model it is determined by making use of glutamine bound X-ray cocrystal of CTPS (PDB code 1VCO) of *Thermus thermophilus* HB8 together with 3NVA in multiple sequence alignment
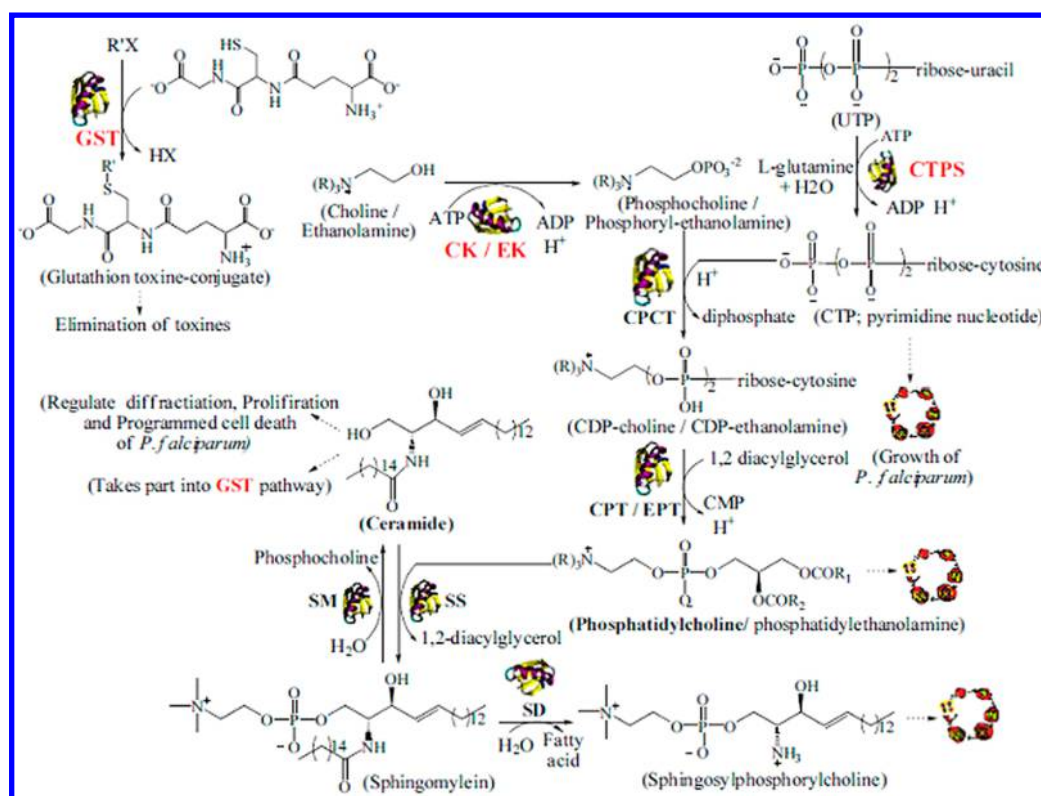
Figure 2. Interconnections between the pathways of CTPS, CK, and GST of *P. falciparum* (CDP, cytidine diphosphate; CMP, cytidine monophosphate; CPCT, choline-phosphate cytidyltransferase; EPCT, ethanolamine-phosphate cytidyltransferase; CPT, cholinephosphotransferase; EPT, ethanolamine phosphotransferase; SS, sphingomyelin synthase; SM, sphingomyelinase; SD, sphingomyelin deacylase).
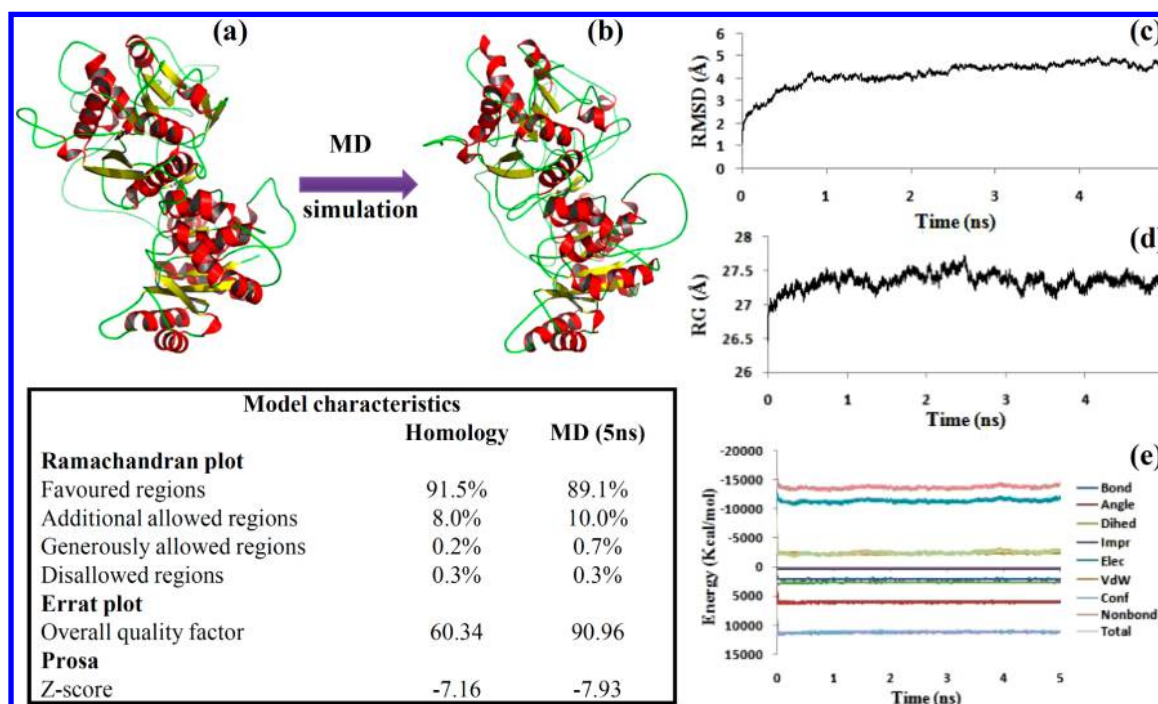

Figure 3. (a) 3D structure of *Pf*-CTPS materialized from CTPS template 3NVA through homology modeling; (**b**) homology model of *Pf*-CTPS at the end of 5 ns molecular dynamics simulations in NAMD; (**c**−**e**) RMSD, radius of gyration, and different components of molecular energy profiles of *Pf*-CTPS trajectories, respectively. The data in the box shows some formal characteristics of *Pf*-CTPS model as developed from homology modeling procedure and after subjecting it to 5 ns MD simulations.

method. This has led to the *Pf*-CTPS's glutaminase site as composed of residues TYR54, GLY384, GLY385, PHE386, CYS412, LEU413, GLN416, GLU435, ARG583, HIS584, ARG585, TYR586, and HIS631.[36] These residues are part of conserved ones in CTPS enzyme from different species. Among these, LEU413, GLU416, GLY385, PHE386, GLU435, and

ARG585 are key residues for interaction with glutamine. Furthermore, the residues MET51 to GLY67 of loop region are part of the gateway for the transfer of ammonia released from the glutaminase domain to the synthetase domain.[36] The results from CASTp, Site-finder of MOE, and protomol of SYBYLX 1.3 also supported the identified pocket.[37,38]

The target sites of remaining two enzymes CK and GST are adopted from their enzyme−ligand cocrystal structure PDB codes 3FI8 and 2AAW, respectively.[39,40] However, the reported 3D structure of CK has gaps at several places. For the purpose of MD simulations the structure is rectified by appropriate modeling techniques. The CK target site residue numbers in the original pdb and rectified pdb are ASP288 (210, residue number in rectified pdb), GLN290 (212), ASP305 (227), GLU307 (229), TYR308 (230), GLU324 (246), TYR329 (251), TRP392 (314), TRP395 (317), TYR414 (336), and ARG418 (340). The GST target site is mainly composed of residues TYR9, GLY14, LYS15, PHE45, GLN58, VAL59, PRO60, GLN71, SER72, GLN104, HIS107, ASN111, PHE116, and TYR211. In CK, among the identified residues, ASP210 and GLN212 play important role in binding the substrate, whereas in GST, the residues TYR9, LYS15, and GLN71 are important for glutathione binding. These target sites are used in virtual screening to identify the CCEs.

3.4. Virtual Screening. In order to acquire the chemical entities for virtual screening (VS) the substrates/inhibitors of the three enzymes were used as query molecules to filter the matching structures from ZINC database. Here, glutamine and 6-diazo-5-oxo-L-norleucine (DON) of CTPS, choline, N-[2-[[3-(4-bromophenyl)-2-propenyl]amino]ethyl]-5-isoquinoline-sulfonamide (H89), and 2-amino-1-butanol of CK, and glutathione, 1-amino-4-{4-({4-chloro-6-[(2-sulfophenyl)-amino]1,3,5-triazin-2-yl}amino)-3-sulfophenyl]amino}-9,10-dioxo-9,10-dihydro-2-anthracenesulfonic acid of GST were used as query molecules (Figure 4).[41−44] The filtering of the ZINC database entries for the VS structures is carried out in conjunction with query molecules (Figure 4) by using the substructure based similarity and "tight filtering" with 50% similarity as search criteria. This has resulted in 8635 molecules for virtual screening (details are in the Supporting Information).
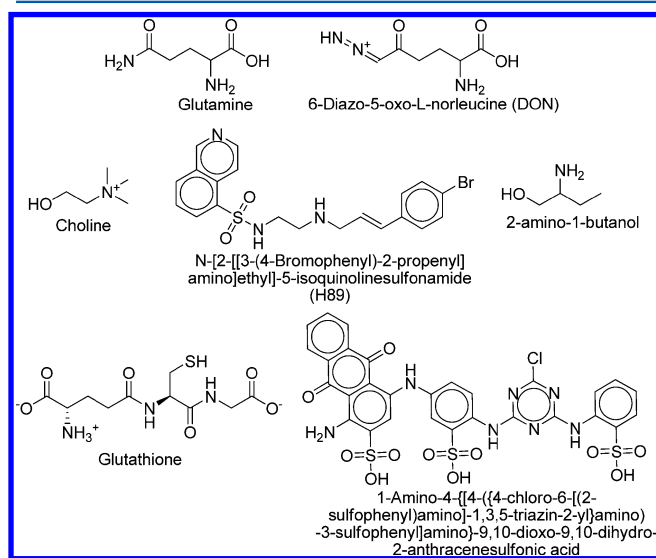
In Surflex-Dock using default settings all these 8635 molecules were screened by docking them in to each target site. For every molecule the best docked pose (for each target) is selected based on its total dock score with due consideration to crash and polar scores. For simplicity only one dock pose, corresponding to maximum total dock score, per molecule is considered. The molecules' total dock scores for each enzyme were analyzed, in conjunction with the total dock scores from remaining two enzymes, by successively arranging them in descending order to identify the chemical entities consensus to all three enzymes. This has led to several ZINC database entries bearing substructures of aryl sulfonamide, aryl sulfonate, aryl acetamide (molecular weight spread 313−470), and peptidomimetics (molecular weight ∼600+) containing glutamine, alanine and/or cysteine moieties, and combinations thereof as agreeable with consensus docking scores to the selected enzymes. From among these, the ZINC entries with substructures of aryl sulfonamide, aryl sulfonate, aryl acetamide are considered in view of their relatively simple scaffolds and low molecular weights. Moreover, the molecular weights of these entries are within the limits suggested by Lipinski's rule of five. In most of these molecules OH, SO_3, SO_2, NH_2, NH, and/or CONH functionalities with aryl groups were found to be involved in binding to the target sites. Briefly, the molecular structures of these ZINC entries represent a functionalized core extended by hydrophobic moieties on one or more sides.

Figure 5 shows the interactions and docking scores of selected ZINC database entries. In *Pf*-CTPS, the SO_2/ SO_3 groups of **ZINC00627448** and **ZINC79315625** showed H-bond with ARG585. In **ZINC49575668**, its SO_2 group showed H-bond with GLY387 of Pf-CTPS. Apart from these the ZINC entries showed H-bonds with MET51, SER52, VAL59, GLY57, GLY385, GLU441, ARG583, and TYR586 through their NH, NH_2, and OH groups. In CK, **ZINC49575668** and **ZINC79315625** interacted with the enzyme through the SO_2/ SO_3 groups by H-bonding with ARG399. In case of **ZINC00627448**, its SO_2 group showed H-bond with GLY114 and ASN117 of the enzyme. The other important residues for H-bonding with NH, NH_2, and OH of ZINC entries are found to be THR116, ASP305, GLN290, GLU307, and TYR308. In GST, the SO_2 group of **ZINC49575668** and **ZINC00627448** showed H-bond with GLN73. In **ZINC79315625**, its SO_3 group showed H-bond with ASP105 of GST. The other key residues for H-bonding with NH, NH_2, and OH of the compounds are found to be LYS15, GLN71, CYS101, and GLN104.

As the ZINC entries selected from the virtual screening are found to interact with the envisaged enzyme targets using their OH, SO_3, SO_2, NH_2, NH, and/or CONH functionalities and aryl moieties, we looked for a scaffold satisfying these features. Also, malaria being an infection prevalent in the lower strata of socio-economic population, its chemotherapy demands compounds from simple and efficient synthetic procedures for exploration. This has led to arylsulfonyloxy acetimidamides, which has high functional similarity with the selected ZINC entries, for exploration. These compounds are easy to synthesize and meet the economic criteria of new drug explorations in malaria chemotherapy.

3.5. Synthesis. The synthesis of target compounds arylsulfonyloxy acetimidamides (**3**) was accomplished using previously reported method.[32] Following Scheme 1, they were synthesized from different 4-substituted benzeneacetonitrailes (**1**). Compound **1** was refluxed with hydroxylamine hydrochloride dissolved in methonolic sodium methoxide for about 12

Figure 4. Query structures used in acquiring the ZINC database entries for virtual screening.
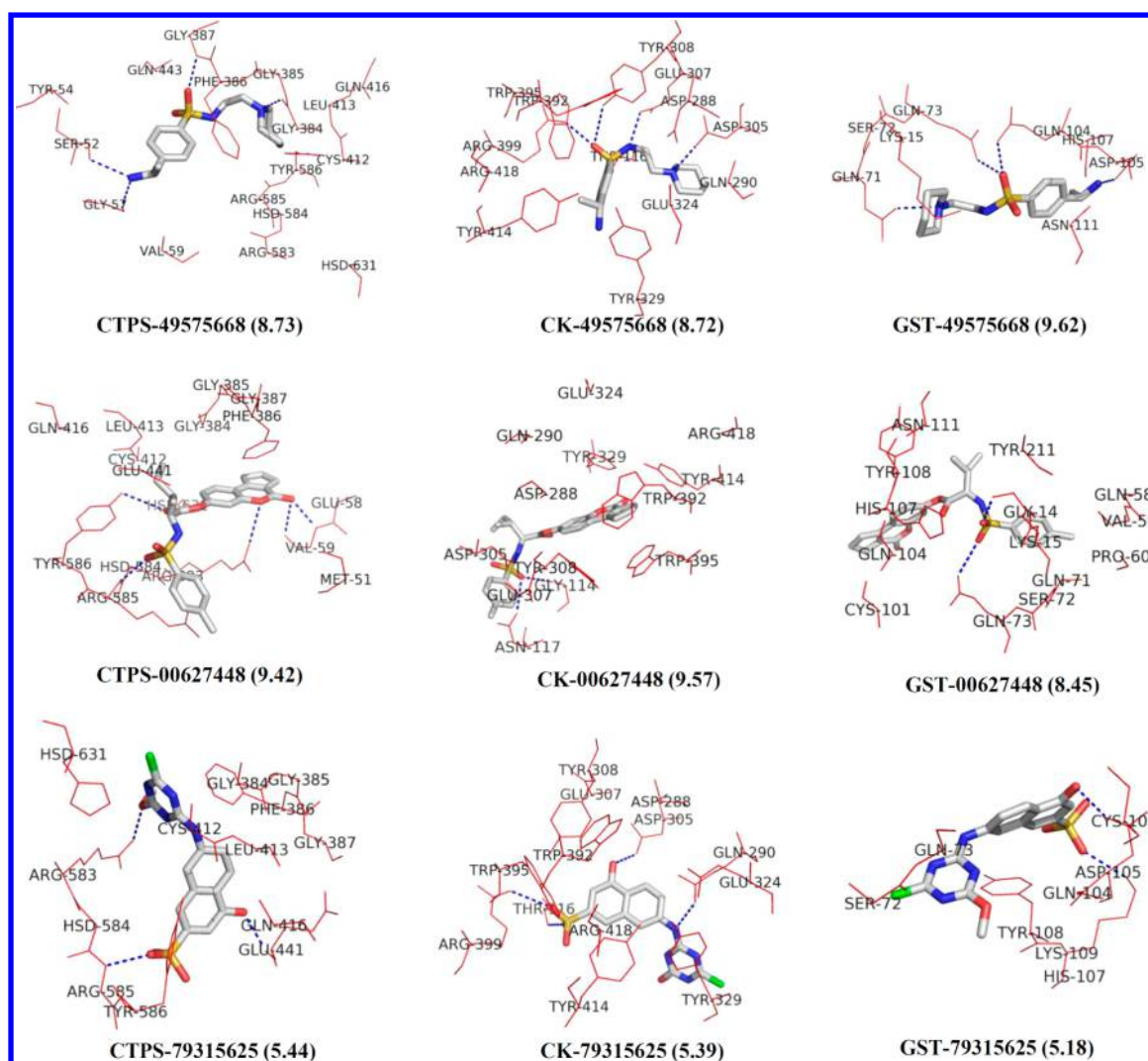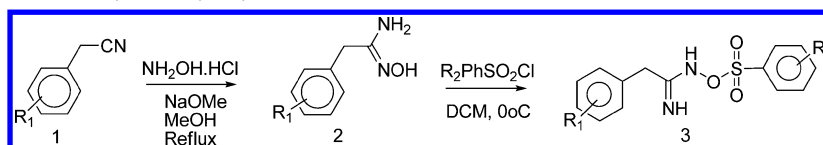
Figure 5. Surflex docked poses of selected ZINC database entries in the target sites of *Pf*-CTPS, CK, and GST with dock scores in parentheses.

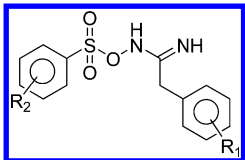**Scheme 1. Synthetic Scheme of Arylsulfonyloxy Acetimidamides**

h to yield corresponding *N'*-hydroxy-2-arylacetimidamide (**2**). This in dichloromethane in the presence of triethayl amine on reaction with arylsulphonyl chloride at 0 °C afforded corresponding arylsulfonyloxy acetimidamides (Table 3) in good yield (70−85%). The compounds were purified by column chromatography and the structures were confirmed by analyzing their ^{1}H and ^{13}C NMR, mass, and HRMS spectra.

3.6. In Vitro Antimalarial Activity and Cytotoxicity. All the compounds (Table 3) were tested for their antimalarial activity against 3D7 (CQ-sensitive) and K1 (CQ-resistant) strains of *P. falciparum* and for cytotoxicity in Vero cell line. Among these, four compounds (**3a**, **3d**, **3e**, and **3h**) showed response against sensitive strain (IC$_{50}$, 1.10−4.36 μM) as well as resistant strain (IC$_{50}$, 2.13−4.28 μM) (Table 3). From these, compounds **3a** and **3d** showed IC$_{50}$ values of 1.10 and 1.45 μM, respectively, against sensitive strain. They also respectively showed IC$_{50}$ values of 2.13 and 3.10 μM against the resistant

strain. The remaining two compounds (**3e** and **3h**) showed IC$_{50}$ values of 3.02 and 4.36 μM against sensitive strain and 3.34 and 4.28 μM against resistant strain. For other compounds the IC$_{50}$ values against one or both the strains is above 5.00 μM. Among these, compound **3o** showed activity only against sensitive strain (IC$_{50}$ = 1.69 μM) and compounds **3b** and **3k** showed activity only against resistant strain (IC$_{50}$, 2.13 and 4.51 μM). In Vero cell line none of the compounds showed any cytotoxicity within the prescribed limits of testing concentrations (10 times the IC$_{50}$ values) (Table 3).

Furthermore, the structures of all synthesized compounds were created in Sybyl-X 1.3 and screened in Surflex-Dock by docking them in each target site following the same protocol as implemented in case of ZINC entries. While the compound's response against 3D7 and K1 strains indicate its net in vitro antimalarial activity, the dock scores for *Pf*-CTPS, CK, and GST indicate its affinity for the respective targets. Since the

Table 3. Arylsulfonyloxy Acetimidamides and Their in Vitro Antimalarial Activity, Cytotoxicity, and Surflex-Dock Scores for *Pf*-CTPS, CK, and GST

| compd | R1 | R2 | IC$_{50}$ (μM)[a] | | CC$_{50}$[b] (μM) | dock score | | |
			3D7	K1		CTPS	CK	GST
3a	*p*-Cl	2,4,6-tri-iPr	1.10	2.10	57.20	6.52	9.17	6.93
3b	*p*-Cl	*p*-CH3	>5.00	2.13	34.00	6.21	6.43	5.40
3c	*p*-Cl	*p*-NO$_2$	>5.00	>5.00	157.50	5.18	5.29	4.84
3d	*p*-OCH$_3$	2,4,6-tri-iPr	1.45	3.10	>200	7.71	7.91	7.13
3e	*p*-OCH$_3$	*p*-CH$_3$	3.02	3.34	>200	7.31	6.73	6.45
3f	*p*-OCH$_3$	*p*-NO$_2$	>5.00	>5.00	>200	7.72	5.82	5.62
3g	3,5-di-Cl	2,4,6-tri-iPr	>5.00	>5.00	117.40	7.27	8.51	5.99
3h	3,5-di-Cl	*p*-iPr	4.36	4.28	54.08	5.59	6.88	6.71
3i	3,5-di-Cl	*p*-CH3	>5.00	>5.00	138.70	6.85	5.97	5.72
3j	3,5-di-Cl	*p*-F	>5.00	>5.00	>200	6.07	5.81	5.62
3k	3,5-di-Cl	*p*-I	>5.00	4.51	>200	5.76	5.88	5.57
3l	3,5-di-Cl	H	>5.00	>5.00	77.33	5.00	6.02	6.47
3m	3,5-di-Cl	*p*-NO$_2$	>5.00	>5.00	125.80	6.29	5.65	4.89
3n	3,5-di-Cl	*p*-OCH$_3$	>5.00	>5.00	>200	6.15	6.48	5.65
3o	*p*-F	*p*-CH$_3$	1.69	>5.00	83.98	6.19	7.29	5.75

[a]3D7, chloroquine sensitive strain; K1, chloroquine resistant strain. [b]Vero cell line.
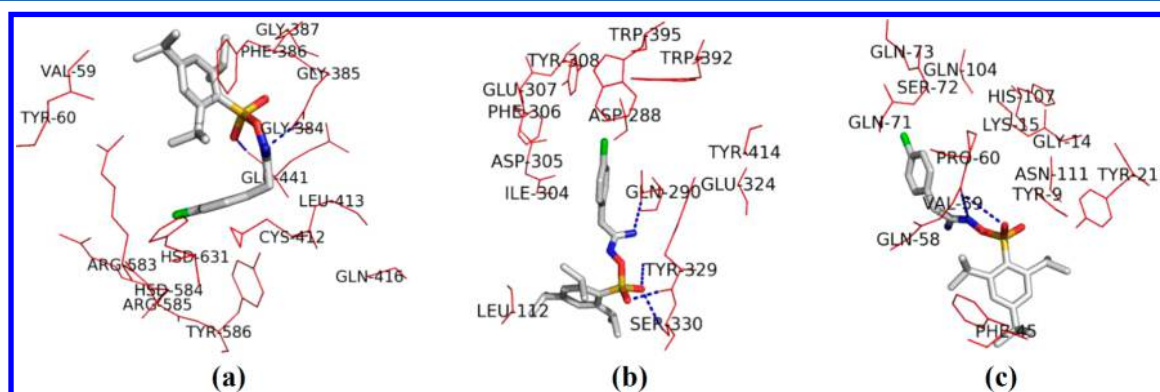
Figure 6. Surflex docked poses of compound **3a** in the target sites of (a) *Pf*-CTPS, (b) CK, and (c) GST.

antimalarial activity of these compounds is expected due to their combined affinity to *Pf*-CTPS, CK, and GST, the cumulative dock scores of these three targets is considered as an index of the in vitro antimalarial activity. The in vitro antimalarial activities of the compounds, excepting **3g**, are in agreement with the cumulative dock scores of the same. On excluding compound **3g**, the correlation between IC$_{50}$ of 3D7 (compounds with IC$_{50}$ > 5.00 are considered as 5.00) and cumulative dock scores of the compounds is 0.69 ($n = 14$, $r^2 = 0.69$); in the case of IC$_{50}$ of K1, it is less but still stands at significant level ($n = 14$, $r^2 = 0.41$). Even though in terms of dock scores compound **3g** appeared very good, in biological test milieu the combination of R1 and R2 groups of this may not be appropriate due to other parameters. Thus, the dock-scores of these compounds with *Pf*-CTPS, CK, and GST are largely in sync with the observed antimalarial activities (Table 3).

Since compound **3a** (Table 3) showed best activity, its docking interactions are analyzed further. Figure 6 shows the docked poses (Surflex) of compound **3a** in the target sites of *Pf*-CTPS, CK, and GST. In *Pf*-CTPS, it has formed H-bonds with the

residues GLY384 and GLU441 through its =NH and =O of SO$_3$ moieties, respectively (Figure 6a). In the case of CK, the compound's =O (of SO$_3$) group formed H-bonds with ASN292, TYR329, and SER330 and the =NH group formed H-bond with GLN290 (Figure 6b). In the target site of GST, the =O of SO$_3$ and NH of compound **3a** showed H-bond interaction with VAL59 (Figure 6c). In spite of best efforts we could not procure/find economical commercial source of selected enzymes; therefore, the compounds could not be tested against them.

3.7. Structure−Activity Relations. The structure−activity profile of the compounds (Table 3) are examined by using the hydrophobicity (π), molar refractivity (MR), and electronic properties (polarity F, resonance R, and Hammett's sigma constant σ_p) of R1 and R2 substituent groups (data provided in the Supporting Information).[45] As the number of compounds with definite activity are limited, the inferences are deduced by comparing molecular pairs sharing common substituent features. The structure−activity profile of these compounds (Table 3) indicate that para-substitution on both the aryl moieties is critical
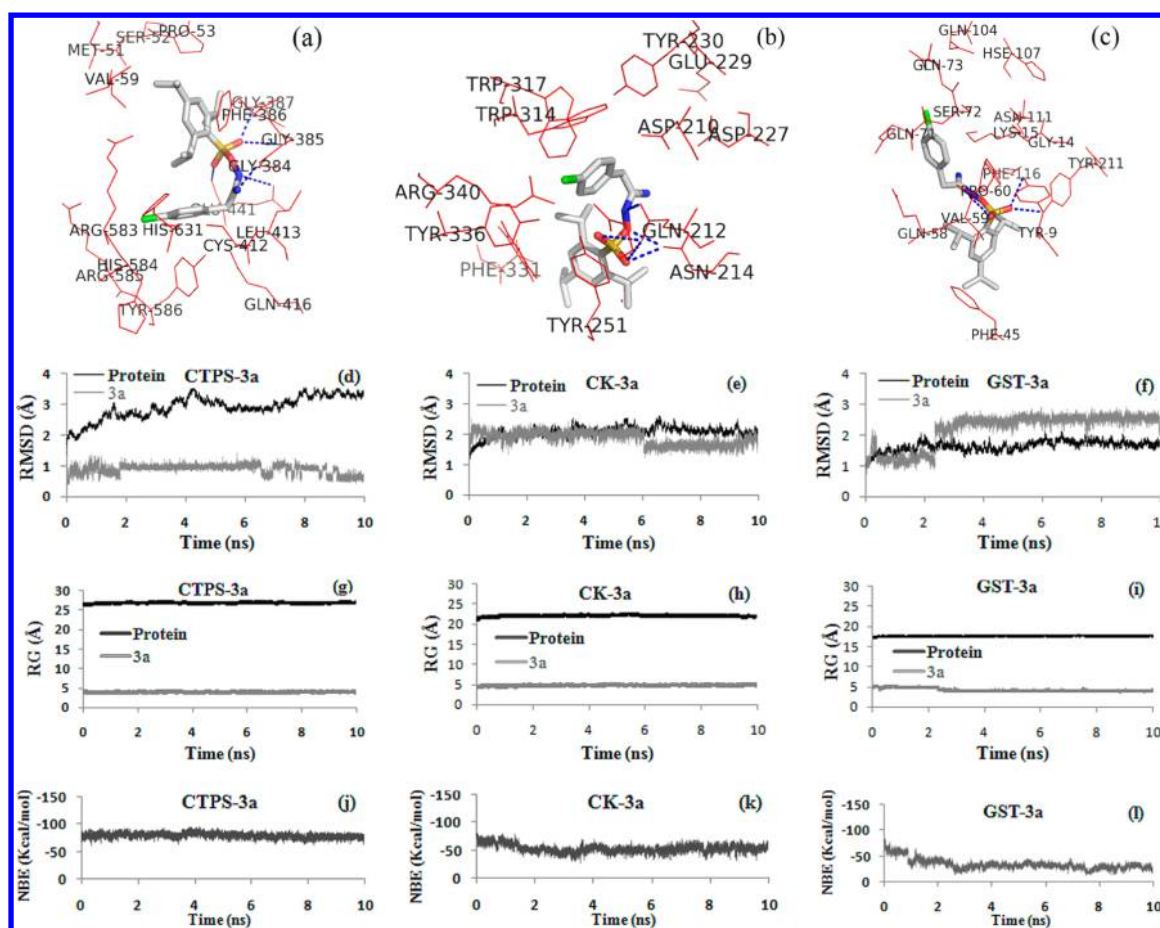
Figure 7. Docking (AUTODOCK) poses of compound **3a** in the target sites of (a) *Pf*-CTPS, (b) CK, and (c) GST, graphs of RMSDs (d−e), radii of gyration (RG) (g−i), and nonbonded interaction energies (NBEs) (j−l) from the MD simulation profile of the *Pf*-CTPS/CK/GST-compound **3a** complex.

for the antimalarial activity against sensitive as well as resistant strains. An examination of the physicochemical characteristics of R1 and R2 groups of the compounds indicated a preference to hydrophobicity (π) and/or molar refractivity (MR) for activity against both the strains (compounds **3a** and **3b** vs **3c**; **3d** and **3e** vs **3f**; **3h** vs **3i**, **3j**, and **3l**−**3n**). Furthermore, the properties (π and/or MR) of R2 substituent(s) showed some degree of cumulative influence on the activity (compounds **3a** vs **3b**; **3d** vs **3e**). Here, **3g** and **3h** are exceptions; it may be that the absence of a para-substitution (R1) on the aryl ring altered the scenario. It is also pointed out that the sensitive strain is more desirous of hydrophobic groups when compared to that of the resistant strain (compounds **3a** vs **3b**; **3d** vs **3e**). Compounds lacking π and/or MR R1 and R2 groups did not show high order of activity in either strain (compounds **3c**, **3f**, **3j**, and **3l**−**3n**). The electronic substituent constants of R1 and R2 groups have not shown a clear trend in inferring the activity profile of the compounds. Nevertheless, this does not rule out their influence on the antimalarial activity of the compounds.

3.8. MD Simulations. Sybyl's Surflex and AUTODOCK are two widely used tools for molecular docking in drug discovery studies. Between these two AUTODOCK is very popular as it is available in public domain and perceived to be very rigorous. With this view we repeated the docking analysis of the most active analogue **3a** (Table 3) and taken it further for molecular dynamics in NAMD. In AUTODOCK, the best docked pose of **3a** resulted in −9.31, −10.88, and −8.65 kcal/mol as binding

energies with *Pf*-CTPS, CK, and GST respectively (Figure 7a−c). Here the top ranked poses of **3a** occupied the same locations of the binding pockets as those from Surflex dock. Furthermore, the docked poses of **3a** in *Pf*-CTPS and GST target sites from Surflex and AUTODOCK showed comparable orientations, but the docked poses of **3a** in CK target site showed some deviation in their orientation (RMSDs between Surflex and AUTODOCK docked poses of **3a** in *Pf*-CTPS, CK and GST are 2.919, 4.587 and 2.861, respectively) (Figures 6 and 7; the superimposed docked poses are provided in the Supporting Information). We have no explanation for the deviation, but it is not unusual in docking exercises. Nevertheless, as in case of Surflex, the docked poses of **3a** from AUTODOCK indicated that =NH and NH of acetimidamide, =O of SO_3 and aryl moieties of the compound (**3a**) play key role in binding to the active sites of the enzymes through one or more H-bonds and/or arene interactions. Some key interactions observed in AUTODOCK poses are described below.

In *Pf*-CTPS, compound **3a** with its =NH, NH (of acetimidamide), and =O of SO_3 moieties anchored on to the binding pocket residues GLY384, GLY387, and GLU441 through H-bonds (Figure 7a). The back bones of GLY384 and GLY387 acted as H-bond acceptor and H-bond donor for =NH and =O of SO_3 moieties of the compound, respectively. The GLU441 with its side chain acted as hydrogen bond acceptor for the NH moiety of the compound. In CK, the compound used its =O of SO_3 moiety for H-bonding with the side chains of

GLN212 and ASN214 (Figure 7b). Apart from this, the chlorobenzene moiety present in compound **3a** showed arene interactions with the indole moiety of TRP317 (Figure 7b). In the docking experiment with GST, compound **3a** showed H-bond interactions with TYR9, VAL59, and TYR211. In this, the side chains of TYR9 and TYR211 acted as hydrogen bond donors for =O of SO_3 moiety, and the backbone of VAL59 acted as hydrogen bond acceptor for NH (of acetimidamide) moiety of the compound (Figure 7c).

While docking studies provide static frames of protein−ligand interactions, the trajectories from molecular dynamics (MD) simulations give scope to investigate the protein−ligand interactions and their energitics during the course of time. Hence, the trajectories of enzyme (*Pf*-CTPS/CK/GST)-compound **3a** complexes from the molecular dynamics (MD) simulations are analyzed to determine the quality of compound's binding and its affinity to the enzymes through their RMSDs from the docked state (Figure 7d−f), radius of gyration (RG; Figure 7g−i), nonbonded interaction energies (NBEs; Figure 7j−l), and intermolecular interactions. The RMSDs of *Pf*-CTPS-compound **3a** and CK-compound **3a** complexes suggest that during entire course of MD simulations, the protein and compound trajectories remained close to each other and retained similarity with their docked orientations (Figure 7d−e). Furthermore, their nonbonded energies remained almost uniform (Figure 7j−k) and RGs confirmed that these systems followed a harmonious swirl throughout the dynamics (Figure 7g−h). For the sake of analysis and discussion of intermolecular interactions, the poses of trajectories of enzyme-compound **3a** complexes were sampled at time intervals of 0.5, 2.0, 3.0, 5.0, 7.5, and 10 ns. The timeline figures of these trajectory poses are provided as part of the Supporting Information. They showed that, in *Pf*-CTPS-**3a** and CK-**3a** trajectories, the compound has maintained many of the prior observed H-bonds with these enzymes.

All through the dynamics of *Pf*-CTPS-**3a** complex, GLU441 has acted as acceptor in anchoring **3a**; GLY384 and GLY387 are other important residues in anchoring **3a** into the target site. In most of the trajectories of *Pf*-CTPS-**3a**, the =O of SO_3 of the compound has shown H-bond interactions with GLU441, GLY385, and GLY387; the NH moiety of the compound also formed H-bond with GLU441. Also, 2,4,6-tri-isopropylbenzene moiety of the compound participated in arene interaction with the PHE386. Apart from these H-bonds, in some other trajectories, the NH moiety of compound **3a** showed hydrogen bond with the backbone of GLY385 of *Pf*-CTPS.

In the MD simulation of CK-**3a** complex, GLN212 is one important residue acted as acceptor as well as donor in anchoring **3a**. In the samples of CK-**3a** trajectories, the =O of SO_3 of the compound showed H-bonds with GLN212 and GLU246. In addition to this, GLN212 showed interaction with the NH moiety of the compound. In some trajectories of CK, the side chain of TYR251 participated in H-bond with NH and =O of SO_3 moieties of compound **3a**. Furthermore, the TRP314 (with its indole moiety) and TYR251 (with its phenyl moiety) have respectively provided arene interactions with the aryl moieties of the compound. The videos of these MD simulations showed that in *Pf*-CTPS and CK, compound **3a** maintained the binding orientation comparable to that of its docked poses in the respective enzymes suggesting the durability and favorability of its interactions with the binding pocket residues.

The picture that emerged from the MD simulation of GST-**3a** complex is somewhat different from that of the *Pf*-CTPS and CK

systems. In a 10 ns MD simulation, the RMSDs of GST-compound **3a** trajectories indicated that while the protein maintained comparable 3D conformation all through the dynamics, the compound showed significant changes in its conformation after 2.5 ns and remained stable thereafter (Figure 7f). Also, the radius of gyration indicated that all through the dynamics the protein trajectories swirled close to each other; whereas, that of the compound showed a clear shift within the binding pocket (Figure 7i). The shift(s) in the compound conformation(s) is also reflected in the nonbonded energies of the system (Figure 7l). As the trajectories of the compound have undergone conformational variations during the simulations, it is also noticed that the compound forming H-bonds with different pocket residues of the protein trajectories. In addition to the prior mentioned interactions, it is observed that the compound's =NH and O= of SO_3 moieties showing hydrogen bonds with GLN58 and ASN111, respectively. Interestingly, in most of the sampled trajectories of GST-**3a**, the compound anchored onto the target site by H-bond with TYR9 and VAL59 through its =O of SO_3 and/or NH functional groups. An examination of the video of the trajectories of GST-compound **3a** complex from MD simulations showed that in the binding pocket the chlorobenzene moiety of the compound flipped during later part of dynamics and remained in that pose until the termination of MD simulation (i.e., 10 ns). Conformational changes in the docked ligands during MD simulations are known in the literature.[46] As the GST-compound **3a** complex showed a fast conformational change after 2.5 ns of MD simulation, a fresh simulation of GST complexed with another docked pose of **3a** (second best docked pose from AUTODOCK) has been carried out for 10 ns to examine the influence of starting pose on the outcome of the results.[47] For this MD simulation all the parameters are kept same as in case of previous GST-**3a** run. We noticed that even though the starting **3a** conformations are different in these experiments, during the course of MD simulation, the conformation of **3a** shifted toward a pose comparable to that of one emerged from previous run. In the second experiment also the chlorobenzene moiety of the compound almost attained same orientation during later part of dynamics (figures and data are in the Supporting Information).

In multitarget approach primarily the drug should be sufficiently tuned to bind to the pathogen's designated enzymes, and at the same time should avoid binding to human proteins. In view of this, the relevance of prototype compound **3a** to *Pf*-CTPS, CK, and GST, in comparison to the matching human proteins, is examined by BLAST search of the respective target sequences (for similarity) and by comparing the docking scores of the compound **3a** against parasite and human targets. An examination of relevant protein sequences of parasite and human revealed that while the binding pocket residues of CTPS and CK are conserved in them, in GST the same are less conserved (<50%). Furthermore, in the BLAST search, the CTPS, CK, and GST from parasite and human sources showed sequence identity between 29 to 38%. These may hint at the dissimilarity of parasite and human proteins. Interestingly, in Surflex-Dock compound **3a** showed higher affinity toward the parasite enzymes when compared to that of human enzymes (Dock scores of *Pf*-enzymes: CTPS, 6.52; CK, 9.17; GST, 6.93. Dock scores of human enzymes: CTPS, 3.74; CK, 5.89; GST, 5.65). These are very preliminary and in vivo studies give the final call on the matter.

These findings collectively suggested that prototype compound **3a** with SO3, =NH, and/or NH functionalities flanked by aryl groups may be critical for binding to *Pf*-CTPS, CK, and GST and suitable for the exploration/development as CCE against the said enzymes. For these systems free energy simulations[48] would have provided more reliable estimates of protein−ligand binding affinities and energetics of conformational changes. However, we could not implement them as they are computationally expensive and beyond our reach. All the same, this prototype compound is worth exploring and may come to use in overcoming the clinical issues associated with routinely used antimalarial drugs.

4. CONCLUSIONS

This study has explored a strategy to design new class of antimalarials through identifying consensus inhibitor against multiple enzyme targets. For this, *Pf*-CTPS, CK, and GST were selected from a database of fifty-six drug targets of *P. falciparum* based on their connectedness and functional importance in biochemical/metabolic pathways. In the absence of 3D structure of *Pf*-CTPS, it has been developed from the FASTA sequence by employing protein structural modeling techniques. The target sites of the selected enzymes were utilized in the virtual screening of chemical structures from ZINC database to identify consensus chemical entity to inhibit them. This has led to the design and synthesis of arylsulfonyloxy acetimidamides as new class of compounds against malaria. Some of these compounds showed good activity against CQ-sensitive (3D7) and resistant (K1) strains of *P. falciparum*. In docking studies these compounds showed binding affinity toward the selected enzymes. Furthermore, the molecular dynamics simulations carried out on these enzymes complexed with compound **3a** ascertained the importance of SO3, =NH, and/or NH functionalities flanked by aryl groups in bind to *Pf*-CTPS, CK, and GST through one or more H-bonds and/or arene interactions. The findings collectively paved the way for arylsulfonyloxy acetimidamides as new class of antimalarial agents. As new chemical scaffolds are urgently needed and are in high demand for the clinical management of malaria, this is a step toward opening a window for the exploration of new antimalarial agents.

■ ASSOCIATED CONTENT

Ⓢ Supporting Information

The Supporting Information is available free of charge on the ACS Publications website at DOI: 10.1021/acs.jcim.5b00392.

Further detail on work flow, druggable enzyme database, selection of target enzymes, structural modeling, virtual screening, synthesis, docking and dynamics, and references (PDF)

Full data corresponding to Tables S8 and S9 (PDF)

MD simulation video of *Pf*-CTPS-compound 3a complex (AVI)

MD simulation video of CK-compound 3a complex (AVI)

MD simulation video of GTS-compound 3a complex (AVI)

MD simulation video of GTS complexed with alternative pose of compound 3a (AVI)

■ AUTHOR INFORMATION

Corresponding Author

*Phone: +91-522-2772450. Fax: +91-522-2771941. E-mail: yenpra@yahoo.com.

Notes

The authors declare no competing financial interest.

■ ACKNOWLEDGMENTS

■ REFERENCES

(1) *World malaria report 2014*; World Health Organization: Geneva, 2014; pp 1−227; http://www.who.int/malaria/publications/world_malaria_report_2014/wmr-2014-no-profiles.pdf.

(2) Flannery, E. L.; Chatterjee, A. K.; Winzeler, E. A. Antimalarial Drug Discovery - Approaches and Progress Towards New Medicines. *Nat. Rev. Microbiol.* **2013**, *11*, 849−862.

(3) Njogu, P. M.; Chibale, K. Recent Developments in Rationally Designed Multitarget Antiprotozoan Agents. *Curr. Med. Chem.* **2013**, *20*, 1715−1742.

(4) Li, K.; Schurig-Briccio, L. A.; Feng, X.; Upadhyay, A.; Pujari, V.; Lechartier, B.; Fontes, F. L.; Yang, H.; Rao, G.; Zhu, W.; Gulati, A.; No, J. H.; Cintra, G.; Bogue, S.; Liu, Y. L.; Molohon, K.; Orlean, P.; Mitchell, D. A.; Freitas-Junior, L.; Ren, F.; Sun, H.; Jiang, T.; Li, Y.; Guo, R. T.; Cole, S. T.; Gennis, R. B.; Crick, D. C.; Oldfield, E. Multitarget Drug Discovery for Tuberculosis and other Infectious Diseases. *J. Med. Chem.* **2014**, *57*, 3126−3139.

(5) White, N. J. Antimalarial Drug Resistance. *J. Clin. Invest.* **2004**, *113*, 1084−1092.

(6) Bloland, P. B. *Drug Resistance in Malaria*; World Health Organization: Geneva, 2001; pp 1−27; http://www.who.int/csr/resources/publications/drugresist/malaria.pdf.

(7) Gardner, M. J.; Hall, N.; Fung, E.; White, O.; Berriman, M.; Hyman, R. W.; Carlton, J. M.; Pain, A.; Nelson, K. E.; Bowman, S.; Paulsen, I. T.; James, K.; Eisen, J. A.; Rutherford, K.; Salzberg, S. L.; Craig, A.; Kyes, S.; Chan, M. S.; Nene, V.; Shallom, S. J.; Suh, B.; Peterson, J.; Angiuoli, S.; Pertea, M.; Allen, J.; Selengut, J.; Haft, D.; Mather, M. W.; Vaidya, A. B.; Martin, D. M.; Fairlamb, A. H.; Fraunholz, M. J.; Roos, D. S.; Ralph, S. A.; McFadden, G. I.; Cummings, L. M.; Subramanian, G. M.; Mungall, C.; Venter, J. C.; Carucci, D. J.; Hoffman, S. L.; Newbold, C.; Davis, R. W.; Fraser, C. M.; Barrell, B. Genome Sequence of the Human Malaria Parasite *Plasmodium Falciparum*. *Nature* **2002**, *419*, 498−511.

(8) Hendriks, E. F.; O'Sullivan, W. J.; Stewart, T. S. Molecular Cloning and Characterization of the *Plasmodium Falciparum* Cytidine Triphosphate Synthetase Gene. *Biochim. Biophys. Acta, Gene Struct. Expression* **1998**, *1399*, 213−218.

(9) Ancelin, M. L.; Vial, H. J. Quaternary Ammonium Compounds Efficiently Inhibit *Plasmodium Falciparum* Growth in Vitro by Impairment of Choline Transport. *Antimicrob. Agents Chemother.* **1986**, *29*, 814−820.

(10) Hiller, N.; Fritz-Wolf, K.; Deponte, M.; Wende, W.; Zimmermann, H.; Becker, K. *Plasmodium Falciparum* Glutathione S-transferase–Structural and Mechanistic Studies on Ligand Binding and Enzyme Inhibition. *Protein Sci.* **2006**, *15*, 281−289.

(11) Schomburg, I.; Chang, A.; Placzek, S.; Sohngen, C.; Rother, M.; Lang, M.; Munaretto, C.; Ulas, S.; Stelzer, M.; Grote, A.; Scheer, M.; Schomburg, D. BRENDA in 2013: Integrated Reactions, Kinetic Data,

Enzyme Function Data, Improved Disease Classification: New Options and Contents in BRENDA. *Nucleic Acids Res.* **2013**, *41*, D764−D772.

(12) Irwin, J. J.; Shoichet, B. K. ZINC−a Free Database of Commercially Available Compounds for Virtual Screening. *J. Chem. Inf. Model.* **2005**, *45*, 177−182.

(13) *SYBYL*, version 7.3; Tripos Associates, St. Louis, MO, 2006.

(14) Morris, G. M.; Huey, R.; Lindstrom, W.; Sanner, M. F.; Belew, R. K.; Goodsell, D. S.; Olson, A. J. AutoDock4 and AutoDockTools4: Automated Docking with Selective Receptor Flexibility. *J. Comput. Chem.* **2009**, *30*, 2785−2791.

(15) Phillips, J. C.; Braun, R.; Wang, W.; Gumbart, J.; Tajkhorshid, E.; Villa, E.; Chipot, C.; Skeel, R. D.; Kale, L.; Schulten, K. Scalable Molecular Dynamics with NAMD. *J. Comput. Chem.* **2005**, *26*, 1781−1802.

(16) Wilkins, M. R.; Gasteiger, E.; Bairoch, A.; Sanchez, J. C.; Williams, K. L.; Appel, R. D.; Hochstrasser, D. F. Protein Identification and Analysis Tools in the ExPASy Server. *Methods Mol. Biol.* **1999**, *112*, 531−552.

(17) Muller, S. A.; Kohajda, T.; Findeiss, S.; Stadler, P. F.; Washietl, S.; Kellis, M.; von Bergen, M.; Kalkhof, S. Optimization of Parameters for Coverage of low Molecular Weight Proteins. *Anal. Bioanal. Chem.* **2010**, *398*, 2867−2881.

(18) Altschul, S. F.; Gish, W.; Miller, W.; Myers, E. W.; Lipman, D. J. Basic Local Alignment Search Tool. *J. Mol. Biol.* **1990**, *215*, 403−410.

(19) Kelley, L. A.; Sternberg, M. J. Protein Structure Prediction on the Web: a Case Study Using the Phyre Server. *Nat. Protoc.* **2009**, *4*, 363−371.

(20) Cole, C.; Barber, J. D.; Barton, G. J. The Jpred 3 Secondary Structure Prediction Server. *Nucleic Acids Res.* **2008**, *36*, W197−W201.

(21) Webb, B.; Sali, A. Comparative Protein Structure Modeling Using MODELLER. *Curr. Protoc. Bioinformatics* **2014**, *47*, 5.6.1−5.6.32.

(22) Linding, R.; Jensen, L. J.; Diella, F.; Bork, P.; Gibson, T. J.; Russell, R. B. Protein Disorder Prediction: Implications for Structural Proteomics. *Structure* **2003**, *11*, 1453−1459.

(23) Marchler-Bauer, A.; Derbyshire, M. K.; Gonzales, N. R.; Lu, S.; Chitsaz, F.; Geer, L. Y.; Geer, R. C.; He, J.; Gwadz, M.; Hurwitz, D. I.; Lanczycki, C. J.; Lu, F.; Marchler, G. H.; Song, J. S.; Thanki, N.; Wang, Z.; Yamashita, R. A.; Zhang, D.; Zheng, C.; Bryant, S. H. CDD: NCBI's Conserved Domain Database. *Nucleic Acids Res.* **2015**, *43*, D222−D226.

(24) Hall, T. A. BioEdit: a User-Friendly Biological Sequence Alignment Editor and Analysis Program for Windows 95/98/NT. *Nucl. Acids. Symp. Ser.* **1999**, *41*, 95−98.

(25) Laskowski, R. A.; MacArthur, M. W.; Moss, D. S.; Thornton, J. M. PROCHECK: a Program to Check the Stereochemical Quality of Protein Structures. *J. Appl. Crystallogr.* **1993**, *26*, 283−291.

(26) Wiederstein, M.; Sippl, M. J. ProSA-Web: Interactive Web Service for the Recognition of Errors in Three-Dimensional Structures of Proteins. *Nucleic Acids Res.* **2007**, *35*, W407−10.

(27) Schuler, L. D.; Daura, X.; van Gunsteren, W. F. An Improved GROMOS96 Force Field for Aliphatic Hydrocarbons in the Condensed Phase. *J. Comput. Chem.* **2001**, *22*, 1205−1218.

(28) Guex, N.; Peitsch, M. C.; Schwede, T. Automated Comparative Protein Structure Modeling with SWISS-MODEL and Swiss-PdbViewer: a Historical Perspective. *Electrophoresis* **2009**, *30*, S162−S173.

(29) Humphrey, W.; Dalke, A.; Schulten, K. VMD: Visual Molecular Dynamics. *J. Mol. Graphics* **1996**, *14*, 33−38.

(30) Pedretti, A.; Villa, L.; Vistoli, G. VEGA−an Open Platform to Develop Chemo-Bio-informatics Applications, Using Plug-in Architecture and Script Programming. *J. Comput.-Aided Mol. Des.* **2004**, *18*, 167−173.

(31) Video match. http://gromada.com/main/download.php (accessed June 16, 2015).

(32) Lin, C. C.; Hsieh, T. H.; Liao, P. Y.; Liao, Z. Y.; Chang, C. W.; Shih, Y. C.; Yeh, W. H.; Chien, T. C. Practical Synthesis of N-substituted Cyanamides via Tiemann Rearrangement of Amidoximes. *Org. Lett.* **2014**, *16*, 892−895.

(33) Singh, S.; Srivastava, R. K.; Srivastava, M.; Puri, S. K.; Srivastava, K. *In-Vitro* Culture of *Plasmodium Falciparum*: Utility of Modified (RPNI) Medium for Drug-Sensitivity Studies using SYBR Green I Assay. *Exp. Parasitol.* **2011**, *127*, 318−3121.

(34) Sharma, M.; Chauhan, K.; Chauhan, S. S.; Kumar, A.; Singh, S. V.; Saxena, J. K.; Agarwal, A.; Srivastava, K.; Kumar, S. R.; Puri, S. K.; Shah, P.; Siddiqi, M. I.; Chauhan, P. M. S. Synthesis of Hybrid 4-Anilinoquinoline Triazine as Potent Antimalarial Agents, their *in Silico* Modeling and Bioevaluation as *Plasmodium Falciparum* Transketolase and *β*-Hematin Inhibitors. *Med. MedChemComm* **2012**, *3*, 71−79.

(35) Lauritsen, I.; Willemoes, M.; Jensen, K. F.; Johansson, E.; Harris, P. Structure of the Dimeric form of CTP Synthase from Sulfolobus Solfataricus. *Acta Crystallogr., Sect. F: Struct. Biol. Cryst. Commun.* **2011**, *67*, 201−208.

(36) Goto, M.; Omi, R.; Nakagawa, N.; Miyahara, I.; Hirotsu, K. Crystal Structures of CTP Synthetase Reveal ATP, UTP, and Glutamine Binding Sites. *Structure* **2004**, *12*, 1413−23.

(37) Binkowski, T. A.; Naghibzadeh, S.; Liang, J. CASTp: Computed Atlas of Surface Topography of Proteins. *Nucleic Acids Res.* **2003**, *31*, 3352−3355.

(38) *MOE*; The Molecular Operating Environment from Chemical Computing Group Inc., Montreal, Quebec, Canada; http://www.chemcomp.com.

(39) Wernimont, A. K.; Pizarro, J. C.; Artz, J. D.; Amaya, M. F.; Xiao, T.; Lew, J.; Wasney, G.; Senesterra, G.; Kozieradzki, I.; Cossar, D.; Vedadi, M.; Schapira, M.; Bochkarev, A.; Arrowsmith, C. H.; Bountra, C.; Weigelt, J.; Edwards, A. M.; Hui, R.; Hills, T. Crystal Structure of Choline Kinase from *Plasmodium Falciparum*, PF14_0020. *PDB*; DOI: 10.2210/pdb3fi8/pdb.

(40) Hiller, N.; Fritz-Wolf, K.; Deponte, M.; Wende, W.; Zimmermann, H.; Becker, K. *Plasmodium Falciparum* Glutathione S-Transferase–Structural and Mechanistic Studies on Ligand Binding and Enzyme Inhibition. *Protein Sci.* **2006**, *15*, 281−289.

(41) Hofer, A.; Steverding, D.; Chabes, A.; Brun, R.; Thelander, L. *Trypanosoma Brucei* CTP synthetase: a Target for the Treatment of African Sleeping Sickness. *Proc. Natl. Acad. Sci. U. S. A.* **2001**, *98*, 6412−6416.

(42) Torres-Rivera, A.; Landa, A. Glutathione Transferases from Parasites: a Biochemical View. *Acta Trop.* **2008**, *105*, 99−112.

(43) Choubey, V.; Maity, P.; Guha, M.; Kumar, S.; Srivastava, K.; Puri, S. K.; Bandyopadhyay, U. Inhibition of *Plasmodium Falciparum* Choline Kinase by Hexadecyltrimethylammonium Bromide: a Possible Antimalarial Mechanism. *Antimicrob. Agents Chemother.* **2007**, *51*, 696−706.

(44) Alberge, B.; Gannoun-Zaki, L.; Bascunana, C.; Tran van Ba, C.; Vial, H.; Cerdan, R. Comparison of the Cellular and Biochemical Properties of *Plasmodium falciparum* Choline and Ethanolamine Kinases. *Biochem. J.* **2010**, *425*, 149−158.

(45) Hansch, C.; Leo, A. In *Substituent Constants for Correlation Analysis in Chemistry and Biology*; Wiley: New York, 1979; Chapter 6, pp 48−63.

(46) Shan, Y.; Kim, E. T.; Eastwood, M. P.; Dror, R. O.; Seeliger, M. A.; Shaw, D. E. How does a Drug Molecule find its Target Binding Site? *J. Am. Chem. Soc.* **2011**, *133*, 9181−9183.

(47) Stjernschantz, E.; Oostenbrink, C. Improved Ligand-Protein Binding Affinity Predictions using Multiple Binding Modes. *Biophys. J.* **2010**, *98*, 2682−2691.

(48) Genheden, S.; Ryde, U. Improving the Efficiency of Protein−Ligand Binding Free-Energy Calculations by System Truncation. *J. Chem. Theory Comput.* **2012**, *8*, 1449−1458.